International Journal of Bifurcation and Chaos, Vol. 28, No. 8 (2018) 1830025 (10 pages)

DOI: 10.1142/S0218127418300252

Anticipated Synchronization and Zero-Lag Phases in Population Neural Models

Germán César Dima
Departamento de Física (Facultad de Ciencias Exactas y Naturales), Universidad de Buenos Aires and IFIBA (CONICET), Intendente Guiraldes 2160, Cuidad Universitaria, Buenos Aires, Argentina
gdima@df.uba.ar

Mauro Copelli
Departamento de Física, Universidade Federal de Pernambuco, Pernambuco 50670-901, Recife-PE, Brazil
mcopelli@df.ufpe.br

Gabriel Bernardo Mindlin
Departamento de Física (Facultad de Ciencias Exactas y Naturales), Universidad de Buenos Aires and IFIBA (CONICET), Intendente Guiraldes 2160, Cuidad Universitaria, Buenos Aires, Argentina
gabo@df.uba.ar

Received March 7, 2018; Revised April 24, 2018

Anticipated synchronization is a counterintuitive synchronization regime between a master and a slave dynamical system in which there is a negative phase difference between the driver and the driven system. By studying a set of simple neural oscillators, we unveil the dynamical mechanisms required to generate this phenomenon. We study master–slave configurations where the slave system is, when uncoupled, in a quiescent excitable state. We exemplify our results by describing the dynamics of a dynamical system proposed to model the part of a songbird's brain involved in song production.

Keywords: Synchronization; average model; neuronal dynamics; nonlinear dynamics.

1. Introduction

Synchronization has caught the attention of physicists since Huygens [1893], and nonlinear dynamicists have worked extensively on this phenomenon for the last years [Pikovsky *et al.*, 2003]. In the field of neuroscience, synchronization was found to be an ubiquitous phenomenon responsible for many effects such as the onset of global oscillations in nervous systems. The conditions needed to achieve synchronization have been investigated from several points of view, ranging from the study of the effects of time delay in the connections [Sun *et al.*, 2017; Sun & Li, 2017; Wang & Chen, 2011; Wang *et al.*, 2008, 2009; Wang *et al.*, 2011] to the coexistence of coherent and incoherent solutions (chimera states) within the network [Bera *et al.*, 2017; Majhi *et al.*, 2016, 2017]. In particular, Voss [2000] reported a specific regime, "anticipated synchronization" (AS), which has attracted much attention in recent years. In this regime, two identical dynamical systems are

connected in a master–slave configuration. Contrary to an unprepared intuition, in the AS regime, the activity of the slave precedes that of the master. One of the original systems proposed by Voss was:

$$\begin{cases} \dfrac{dx}{dt} = f(x(t)), \\ \dfrac{dy}{dt} = f(y(t)) + K(x(t) - y(t-\tau)), \end{cases} \tag{1}$$

which has a solution

$$y(t) = x(t+\tau). \tag{2}$$

This led Matias *et al.* [2011] to extend these ideas to neuroscience, exploring biologically plausible neural architectures where some feedback mechanism would play the role of the delayed term in the paradigm of Voss. They explored in particular two different motifs. In the first one, a "master" excitatory neuron was unidirectionally coupled to a "slave" excitatory neuron, which in turn was coupled to an inhibitory neuron that fed back to it. In the second motif, a global driver forced this same architecture. In both cases, the authors placed the neuron models in a periodic regime and found that the master and the slave could phase lock. In that context, the difference between AS and delayed synchronization (DS) lies simply on the sign of the locked phase difference: in AS (DS) the spike of the slave is closest to the succeeding (preceding) spike of the master.

What is surprising about this phenomenon is that if a neuron is in its quiescent state, it needs the master to spike to initiate the chemical processes leading to the generation of an action potential. This can easily lead one to expect that no spike can occur without a previous spike of the master, disregarding that if the slave system operates in a periodic regime, its internal dynamics can sustain continuous spiking even if the driver is turned off. In this way, AS defies a naive expectation in terms of causality: we tend to interpret each nonspiking neuron as if it is in its quiescent state, disregarding that the other variables determining its dynamics might place it in a different dynamical state.

Many neural arrangements involve unidirectional coupling between different populations. Moreover, these architectures are present in motor pathways, which are frequently involved in the generation of repetitive, recurrent patterns [Nottebohm *et al.*, 1976]. Therefore, it is plausible to find this puzzling dynamics where unidirectional connections sustain, eventually after some transient, the synchronization between different areas. Again, what makes the observation challenging is that, in many cases, these motor patterns are studied by means of extracellular recordings, making the spikes the only observable signatures of the dynamics. In fact, this might lead to misinterpreting causality as synonymous with upstream spikes preceding downstream ones (as it would be, in fact the case, if a downstream area was at its quiescent state). Yet, many behaviors imply recurrent, periodic dynamics, where these conditions are not met, and therefore a phenomenon such as AS is possible. This is the main topic of this work.

Motor pathways are involved in the generation of the patterns that drive the peripheral systems in charge of the interaction between an individual and its environment. Therefore, its output is naturally described in terms of the average activity. In many cases, models for the average activity of the different neural populations that constitute a motor pathway are phenomenological in nature. It is not always possible to write detailed models for neural circuits. The number of neurons involved, as well as the difficulty of unveiling the structure of the *connectome*, attempt against the efforts. It is for those reasons that many systems are described in terms of simpler population (rate) models.

Additive models are an example of this approach. Moreover, a recurrent neural motif found in motor pathways is the neural oscillator; an interconnected set of excitatory and inhibitory populations of neurons capable of displaying a rich variety of behaviors, oscillations among them. Other possible dynamics displayed by this architecture is excitability: an asymptotic stationary state towards which the system might converge through qualitatively distinct trajectories.

In this work we proceed to extend previous results concerning AS in two directions. First, we will look for AS in models designed to describe the evolution of a neural population's average activity, instead of in models of simple circuits built from individual neurons. Second, we are interested in exploring the anticipated regime when the slave, when uncoupled, is in an excitable regime. In the original work on AS, both the slave system and the driver display autonomous oscillations if the coupling is neglected. To carry out these extensions, we performed a series of computational studies in a

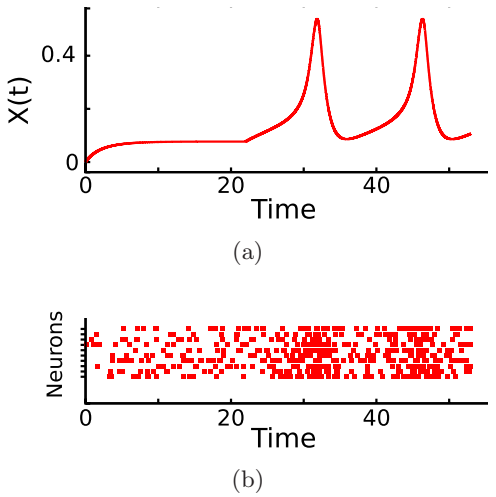

Fig. 1. Variables of rate models in terms of single activity: (a) Average models provide statistical information about firing rates and do not inform on the particular firing pattern of a single neuron. Near zero activity in this representation should be interpreted as low activity rate and (b) as shown in the raster plots, higher rates of firing neurons are translated in the rate model as amplitude peaks.

set of progressively simpler systems, with the final objective of unveiling the minimal ingredients that are needed to reproduce the phenomenon.

Our description of the neural architectures being studied is carried out in terms of average (rate) models [Wilson & Cowan, 1973; Hoppensteadt & Izhikevich, 2012]. We illustrate how to interpret the variables of our description in Fig. 1. In Fig. 1(a), X stands for the rate of activity in a neural population, while Fig. 1(b) shows a raster plot of ten neurons whose spiking is consistent with the variable $X(t)$ in Fig. 1(a). In this way, our dynamical unit is a population of interconnected neurons whose average activity is the target of our modeling effort.

2. A Classical Motif

The motivating problem proposed by Voss [2000], involved two units coupled with an explicit time delay. Matias *et al.* [2011] built their first neural motif mimicking those ingredients. They coupled two neural oscillators to a third unit, inhibitory in nature. In this way, the time-delayed negative feedback was provided by this interneuron, projecting back to the slave system.

In our first model, we built an architecture consisting of a master and a slave (i.e. with an unidirectional coupling). The master is a neural oscillator (i.e. a phenomenological dynamical system representing the dynamics of two neural populations, one excitatory and one inhibitory), operating in a region of the parameter space for which there are oscillations. The slave consists of an excitable system, built with one excitatory population and two inhibitory ones. The rationale for this architecture is that it ultimately mimics the original configuration; we have two neural oscillators with unidirectional coupling, with the slave one bi-directionally connected to an inhibitory population, while the original motif consisted of two periodically spiking units, with the slave coupled to an inhibitory neuron. Notice that in our example, the driven slave system operates at the excitable regime. In other words, if the coupling with its master is eliminated, the slave converges to its quiescent state. In Fig. 2(a), we show the basic architecture, while in Fig. 2(b) we display the dynamics of the driver and the slave in the absence of coupling between them. The equations ruling the dynamics of the system read as [Wilson & Cowan, 1973; Hoppensteadt & Izhikevich, 2012]:

$$\begin{cases} x'_m = -x_m + S(-3.1 + 10x_m - 10y_m), \\ y'_m = -y_m + S(-7.0 + 10x_m + 3y_m), \end{cases} \tag{3}$$

$$\begin{cases} x'_s = -x_s + S(-3.5 + 10x_s - 10y_s \\ \qquad + g_e x_m - g_i z_s), \\ y'_s = -y_s + S(-8.0 + 10x_s + 3y_s), \\ z'_s = -z_s + S(-4.0 + 3z_s + 7x_s), \end{cases} \tag{4}$$

where (x_m, y_m) stands for the activities of the master, (x_s, y_s, z_s) for the activities of the slave, and nonlinearity comes from the sigmoidal function $S(x) = (1 + \exp(-x))^{-1}$. The values of the parameters were chosen so that the driver displays oscillations, and the slave is at its quiescent (excitable) state if $g_e = 0$.

We integrated the equations of this model for different values of the parameters g_e, g_i, and summarized our results in the diagram displayed in Fig. 2(c). The region at the left (blue) corresponds to what we call delayed synchronization (DS). This is a phase locked regime in which the preceding maxima of the master are closest to the maxima of the slave. For higher values of the excitatory coupling, the system converges to a periodic regime for which the succeeding maxima of the master are closest to the maxima of the slave. This is known as the anticipated synchronization regime (AS). These two

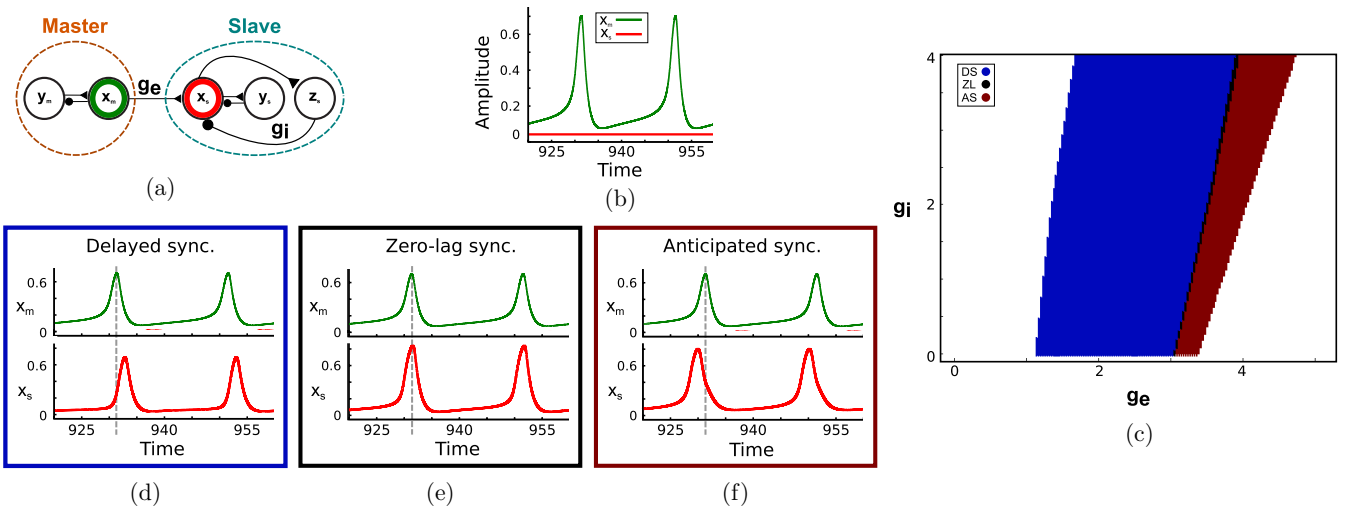

Fig. 2. Anticipated synchronization in a Master–Slave-Interneuron rate model: (a) The driving system (master) is modeled by means of two populations of excitatory and inhibitory neurons (x_m and y_m). The driven system (slave) has the same internal structure, but it presents an additional inhibitory population z_s coupled to the excitatory set x_s, through an inhibitory coupling g_i. The master drives the slave system with a strength factor g_e, (b) the constants of the model were chosen in such a way that the master displays an oscillatory dynamics and, in the absence of coupling ($g_e = 0$) the slave system remains at its quiescent (excitable) state, (c) by varying the values of g_e, g_i, we studied the regions where the peaks of amplitude of x_s are achieved a time after the maxima activity of x_m (DS, blue region) and before the maxima activity (AS, brown region). These two states are separated by a curve (ZL, black region) where both peaks present their maxima at the same time. The three states are displayed in panels (d)–(f).

open regions of the parameter space are separated by a curve for which the maxima coincide. We refer to this regime as zero-lag synchronization (ZL). These three regimes are displayed in Figs. 2(d)–2(f). Other regions of the parameter space allow us to find more involved dynamics; one for which subharmonic responses are found. There is an extensive literature on the dynamics of forced excitable units [Aihara *et al.*, 1984; Coombes *et al.*, 2001], and we do not discuss these solutions in this work.

3. A Simple Neural Oscillator

In order to unveil the dynamics behind this phenomenon, we are going to revisit other (simpler) architectures, testing the hypothesis whether they are capable of displaying the phenomenon. In this section, we are going to explore the behavior of two neural oscillators, each described by the Wilson–Cowan model [Wilson & Cowan, 1973]. A neural oscillator consists of an excitatory population coupled to an inhibitory one. They are further connected in a master–slave configuration, as shown in Fig. 3(a). The dynamics displayed by each neural oscillator is shown in Fig. 3(b). Notice that depending on the parameter values, it can be oscillatory, stationary, or even [in the region labeled II in Fig. 3(b)] excitable. Figure 3(c) shows the behavior of each of the two neural oscillators when uncoupled. The slave is a neural oscillator whose parameter values are set so the system exhibits excitable dynamics. The equations describing this configuration are:

$$\begin{cases} x'_m = -x_m + S(\rho_x^m + 10x_m - 10y_m), \\ y'_m = -y_m + S(\rho_y^m + 10x_m + 3y_m), \end{cases} \tag{5}$$

$$\begin{cases} x'_s = -x_s + S(\rho_x^s + 10x_s - 10y_s + g_e x_m), \\ y'_s = -y_s + S(\rho_y^s + 10x_s + 3y_s + g_i x_m), \end{cases} \tag{6}$$

whereas in the example of the previous section the variables (x_m, x_s) stand for the excitatory activities of the master and the slave, and (y_m, y_s) represent the inhibitory activities. The parameters measure the intensity of the coupling between the excitatory population of the master and the excitatory and inhibitory populations of the slave, respectively. As described above, the constants in the equations were chosen so that the master behaves periodically ($(\rho_x^m, \rho_y^m) = (-3.1, -7.0)$), and the slave displays excitable dynamics before the coupling ($(\rho_x^s, \rho_y^s) = (-3.6, -7.0)$).

We explored the solutions of this model for different values of g_e, g_i, and the results are

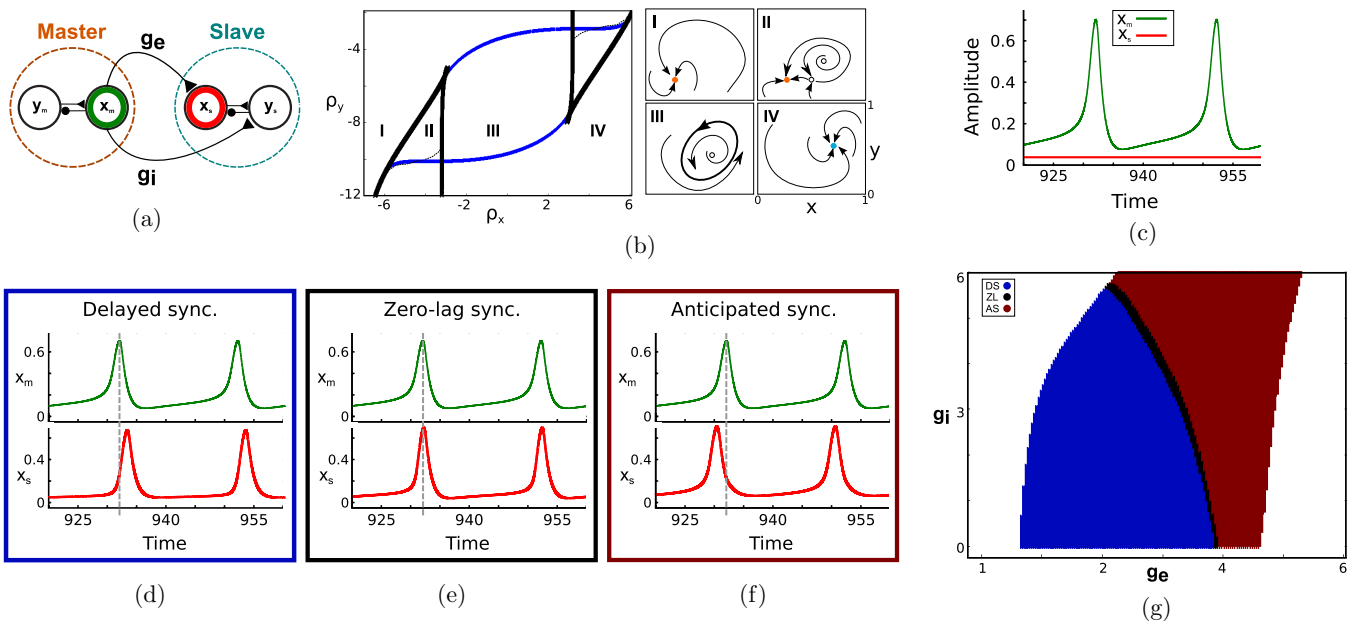

Fig. 3. Anticipated synchronization in a simple neural oscillator: (a) Both the master and the slave systems are represented by two coupled populations of excitatory and inhibitory neurons (x_m and y_m for the driver system and x_s and y_s for the driven system). An unilateral connection is made between x_m and both sets of the slave with weights g_e and g_i, (b) both systems are described using Wilson–Cowan rate models. By tuning the internal constants of the model (ρ_x, ρ_y) it is possible to achieve qualitatively different dynamics, such as displayed in the phase diagram. The regions correspond to: (I) quiescent state, (II) excitable regime, (III) spiking regime and (IV) constant activity. These dynamics are separated by a SNILC (blue line) and an Andronov–Hopf bifurcation (black line). A homoclinic separatrix is sketched with a dashed line, (c) the master's parameters are set to be in the region III whereas the slave is set, in the absence of coupling ($g_e = 0$ and $g_i = 0$), to be in region II. Different dynamics, including (d) DS, (e) ZL and (f) AS can be achieved by (g) tuning both coupling strengths.

summarized in Figs. 3(d)–3(g), where we painted with different colors the parameters leading to delayed synchronization, zero-lag synchronization and anticipated synchronization. Notice that for a constant g_i, the system presents AS as we increase the value of g_e. Let us inspect the parameter space displayed in Fig. 3(b). The slave is (for zero coupling) in what is labeled as region II of the parameter space, where the system is excitable, with an attractive fixed point close to a saddle fixed point that is connected with a repulsor by its stable manifold. This invariant curve separates the space into regions where transients will converge to the attractor through qualitatively different paths. When we consider the modification of the dynamics that occurs as the slave is connected to the driver, we notice that the effect of large g_e will be to place the slave into a region of the parameter space where (if g_i was constant) the oscillations of the slave would present high frequencies. This provides a clue on the minimal dynamical ingredient that we need in order to have AS, and we will implement a last dynamical caricature to validate our hypothesis.

4. A Dynamical Caricature

The success of finding this phenomenon in a simpler Wilson–Cowan model inspired us to search for a minimal dynamical system, consisting of an Adler's equation driven by a periodic signal [Fig. 4(a)]. In this case, the driver is represented by an angular variable rotating at constant speed, while the driven slave system is represented by an angular variable whose dynamics displays a saddle node. The model can be written as:

$$\begin{cases} \theta'_m = \omega_1, \\ \theta'_s = \omega_2 + \varepsilon \sin(\theta_s) + k \sin(\theta_m - \theta_s). \end{cases} \tag{7}$$

The dynamics of the driven system, in this way, can present a wide range of frequencies. Without coupling ($k = 0$), the slave will present excitable dynamics when $\omega_2 < \varepsilon$ [Fig. 4(b)]. This is the regime that we explored, for different values of ω_2. We constrained our simulations to values of the detuning $\chi = \omega_2 - \omega_1$ that would lead to phase locked behavior. The different regions of the parameter space leading to delayed synchronization,

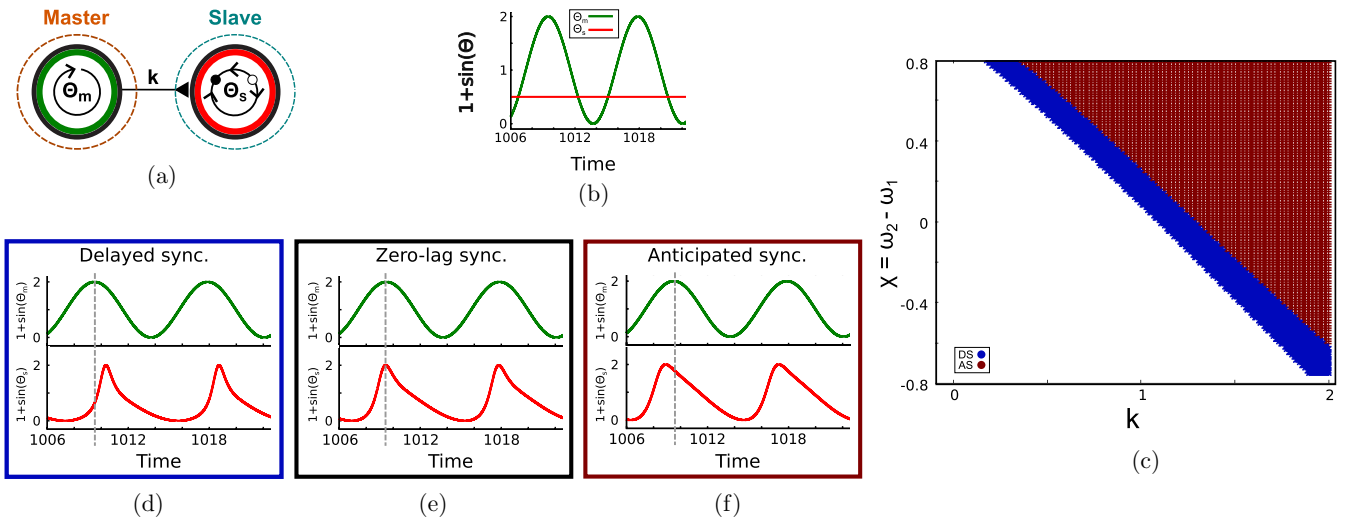

Fig. 4. Anticipated synchronization in theta neurons: (a) In order to unveil the basic mechanisms responsible for AS, a simple theta neuron oscillator system is presented. The slave system is represented by its phase dynamics θ_m oscillating at a constant frequency ω_1. The slave system is modeled by an Adler oscillator θ_s, with a self frequency ω_2. An unilateral coupling between the master and the slave systems is added, with strength, (b) when $k = 0$, the slave system displays an excitable dynamics, (c) different values of the detuning ($\chi = \omega_2 - \omega_1$) and coupling results in (d) DS regime, (e) ZL synchronization and (f) AS. All the simulations were made using fixed values of $\varepsilon = 1.5$ and $\omega_1 = 0.75$.

zero-lag synchronization and anticipated synchronization, are shown with different colors, as well as examples of simulations carried out for parameters in each region, in Figs. 4(c)–4(f).

The inspection of the parameter space of the system allows us to understand the dynamics behind this phenomenon. Notice that the AS region is found, for each value of the detuning, for coupling values higher than a threshold. In other words, when the forcing takes the driven system away from its quiescent state to regions of the parameter with periodic dynamics, it can carry it to regions where the driven's autonomous dynamics would move faster than the driver. In this way, the driven system can display a peak of its activity simultaneously or even before the driver presents its peak. In other words, the key element, from a dynamical point of view, for having zero-lag or AS in a master–slave configuration is the capacity to drive the system towards a region of the parameter space where the dynamics of the slave is faster than that of the driver.

5. About Anticipated Synchronization and Causality

One feature of the presented models is the ability to synchronize with almost no need of a transient time. Figure 5(a, top) shows the slave system anticipating the master's maximum of activity already at the first spike. This behavior could easily be misinterpreted in terms of causality. Nevertheless, it is important to recall that rate models capture the activity of several neurons. Figure 5(a, bottom) shows simulated raster plots of the spikes of several neurons that could lead to the rate curves atop. The neurons in the master system recruit the ones in the slave system (i.e. the spiking activity in the master is nonzero prior to the maximum in the average rate model). The phenomenon of AS is achieved when the activity of the master's excitatory neurons is enough to lead to a maximum spike rate of the slave system, but before reaching the maximum activity of the master's neurons. Another example of the hidden variables of the rate model which are responsible for AS is shown in Fig. 5(b), where the master system is also placed in a region of excitability of the parameter space. The master is then perturbed from its equilibrium by a short pulse, weak enough not to induce a spike of the master population. However, this activity is enough for the slave system to surpass the threshold of excitability and to display a large excursion in the phase space.

6. A Circular Model for the Song System

Birdsong production is the behavioral emergence of a set of specialized regions of the avian brain. The complete architecture of the song motor pathway is

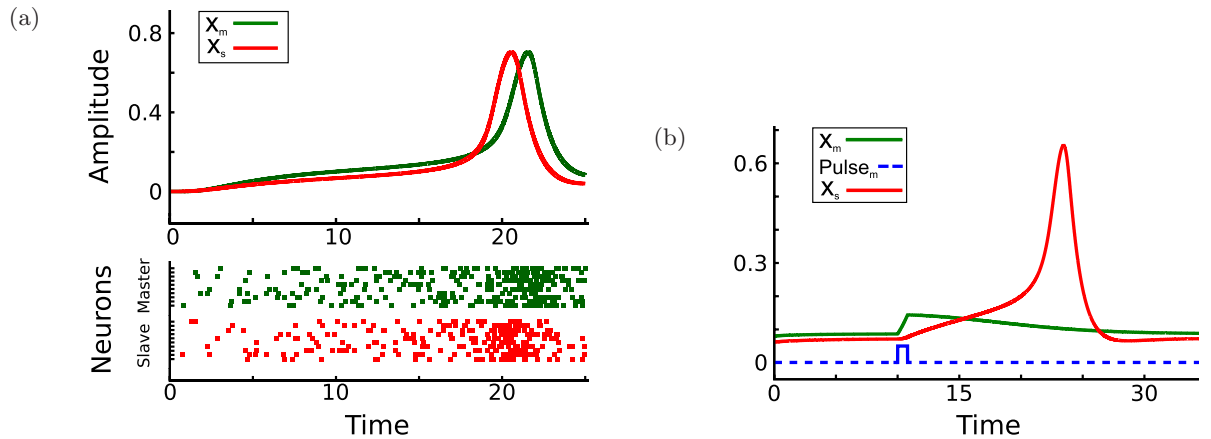

Fig. 5. Causality in terms of rate models: (a) In the framework of average models, having the maximum of amplitude of the slave system occurring before the master's peak of activity can lead to a misunderstanding in terms of causality. The increase of amplitude should be interpreted as an increase of firing rate, and the focus should not only be placed at the time of the spike. As shown in the raster plots, as the average activity of the master starts to rise, it starts to recruit more neurons from the slave system. However the spiking rates of the slave system is faster than the master's, that ultimately leads to the AS phenomenon and (b) this could lead to cases where the master's activity is subtle (for example, by being moved from its equilibrium by an external pulse) but enough to start a chain of activations in the slave system.

still an open question, but it has been well established that there are brain areas which are connected in a feed-forward way, such as the telencephalic nuclei HVC (proper name) and RA (robust nucleus of the arcopallium) [Ashmore *et al.*, 2005].

In the direction of unveiling this motor circuit, an increase in the activity of HVC at significant motor instances, such as the initiation of syllables, was reported in [Amador *et al.*, 2013]. Moreover, the work of other groups reported a

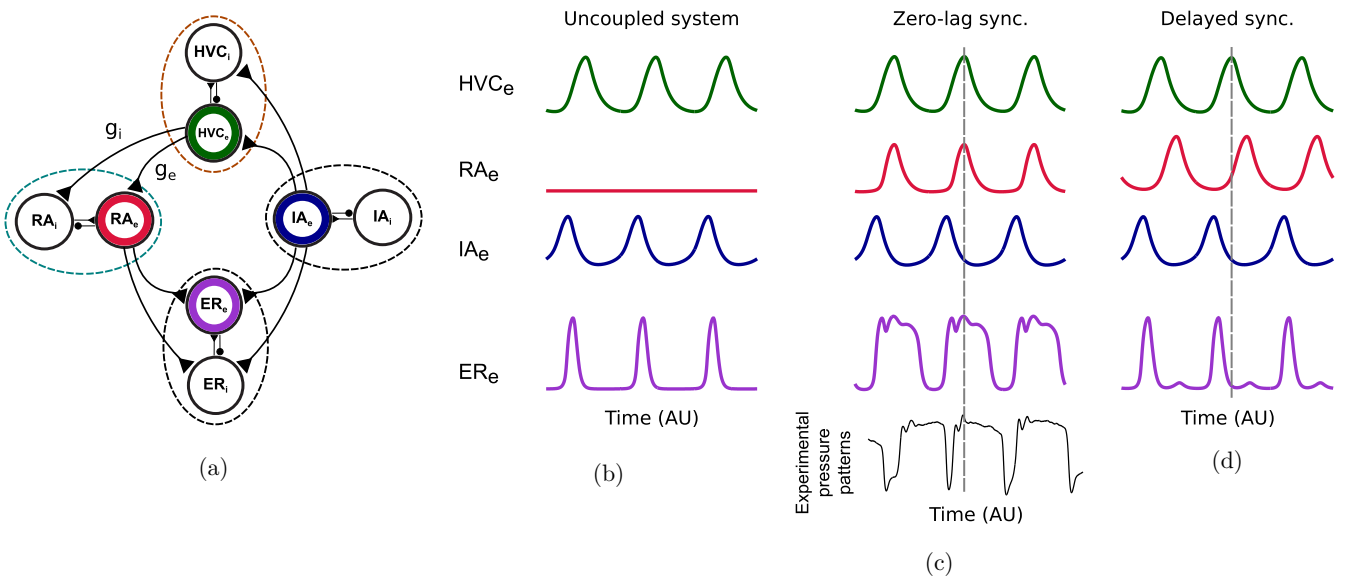

Fig. 6. A birdsong circular neural model capable of displaying AS: (a) An anatomically plausible neural model based on the master–slave structure of Fig. 1. The Initiating Area system (IA) periodically drives both the respiratory area (ER) and the thelencephalitic area HVC. This nucleus projects to RA with coupling strength g_e and g_i. Finally, the loop is closed with a direct connection between RA and ER. The respiratory gestures, therefore, are composed with the contribution of both IA_e and RA_e, (b) in the absence of coupling in the top-down pathway ($g_e = 0$ and $g_i = 0$), RA remains in an excitable state and ER displays a simple oscillatory structure, (c) however when the coupling strength parameters are tuned to display ZL between HVC and RA, the dynamics in ER resembles experimental pressure patterns. Note that the maximum activity in HVC is synchronous with the second peak in the pressure patterns and (d) if the dynamics in RA is delayed from the one in HVC, a simpler structure in the respiratory area is recovered.

similar phenomenon in juvenile zebra finches [Okubo *et al.*, 2015]. This led to a heated debate in the birdsong community, where part of the argument relies on whether regions of the brain connected in a feed-forward fashion can display simultaneous bursts of activity. We propose to test theoretically the hypothesis that it is plausible to have zero-lag activity between brain regions arranged in an architecture involving causally related areas.

We propose a simple neural architecture based on the work of Alonso *et al.* [2015]. This model involves several areas that play a key role in the song generation (as lesions on them would stop the behavior). Each of these areas is modeled by neural oscillators such as the ones presented in the previous sections. The circuit reads as follows: Within the brainstem, an unallocated region (Initiating area, IA) drives a respiratory related area (ER) that is used as a proxy to the pressure patterns in the air sacs. IA also projects to HVC. The processed information in HVC flows top-down back to the brainstem via RA. The complete motor gesture is therefore obtained by the integration of the direct input of IA to ER and the processed signal arriving from the telencephalon [Fig. 6(a)]. The equations used in the model (which are based on the work of Alonso *et al.* [2015]) are:

$$\begin{cases} \mathrm{IA}'_e = 40(-\mathrm{IA}_e + S(-2.7 + 10\mathrm{IA}_e - 10\mathrm{IA}_i)), \\ \mathrm{IA}'_i = 40(-\mathrm{IA}_i + S(-6.8 + 10\mathrm{IA}_e + 3\mathrm{IA}_i)), \\ \mathrm{HVC}'_e = 40(-\mathrm{HVC}_e + S(-4.0 + 10\mathrm{HVC}_e \\ \qquad - 10\mathrm{HVC}_i + 2.7\mathrm{IA}_e)), \\ \mathrm{HVC}'_i = 40(-\mathrm{HVC}_i + S(-8.2 + 10\mathrm{HVC}_e \\ \qquad + 3\mathrm{HVC}_i + 1.7\mathrm{IA}_e)), \\ \mathrm{RA}'_e = 40(-\mathrm{RA}_e + S(-3.5 + 10\mathrm{RA}_e \\ \qquad - 10\mathrm{RA}_i + g_e \cdot \mathrm{HVC}_e)), \\ \mathrm{RA}'_i = 40(-\mathrm{RA}_i + S(-7.9 + 10\mathrm{RA}_e \\ \qquad + 3\mathrm{RA}_i + g_i \cdot \mathrm{HVC}_e)), \\ \mathrm{ER}'_e = 130(-\mathrm{ER}_e + S(-7.5 + 10\mathrm{ER}_e \\ \qquad - 10\mathrm{ER}_i + 7.6\mathrm{IA}_e + 5.0\mathrm{RA}_e)), \\ \mathrm{ER}'_i = 130(-\mathrm{ER}_i + S(-11.5 + 10\mathrm{ER}_e \\ \qquad - 2\mathrm{ER}_i + 3.5\mathrm{IA}_e + 0.6\mathrm{RA}_e)), \end{cases} \tag{8}$$

where the subscript denotes the nature (excitatory/inhibitory) of the labeled population. The constants were chosen such that IA displays a periodic activity. The rest of the areas present an excitable dynamics. The parameters g_e, g_i denote the coupling strength between the excitatory population in HVC and the excitatory and inhibitory populations in RA respectively. If the coupling is eliminated, the respiratory patterns display only the response of IA activity [Fig. 6(b)].

In terms of timing, it is intuitive to think that each area involved in the process would add a time delay compared to the previous connected area. Therefore the information going to ER by the top-down path would be delayed from the activity in HVC. As previously studied, it is possible to achieve zero-lag synchronization between HVC and RA by tuning g_e, g_i. As shown in Fig. 6(c), the maximum activity in HVC_e correlates with a maximum of the generated pressure pattern. The dynamics in ER_e recovers the features of experimentally obtained pressure patterns during the production of song syllables. Moreover, if the system presents DS, the respiratory patterns show a dynamics similar to the one with $(g_e, g_i) = (0, 0)$ [Fig. 6(d)].

7. Conclusions

In this work, we built on previous findings, showing that anticipated synchronization can be found in average rate models of neural activity. Moreover, we have shown that this phenomenon can occur even if the slave is tuned to excitability (a result reminiscent of what has recently been reported for a motif of three excitable neurons under the influence of noise [Matias *et al.*, 2016]). By progressively studying simpler architectures, we built very simple dynamical systems showing the phenomenon, allowing us to identify its minimal dynamical ingredients. We have shown that the slave has to be able to be pushed into a region of its parameter space where its autonomous dynamics would present a frequency higher than the driver's one. Our results are in agreement with previous reports on coupled oscillators in chaotic regimes displaying AS [Pyragienė & Pyragas, 2013].

We showed that in a recently proposed model of the oscine brain song system [Alonso *et al.*, 2015; Dima *et al.*, 2018], this phenomenon allows finding zero-lag between causally related, feed-forward nuclei. This challenges the expectation that causally related brain areas have to display delayed synchronization. Recent observations such as the simultaneity between syllabic onset and HVC activity in

juvenile vocalizations [Okubo *et al.*, 2015] can be interpreted in the framework of zero-lag synchronization, as discussed in this manuscript. The coordination of activity in distant regions of a neural architecture might be fundamental in the process of learning, as zero-lag has been shown to be an attractive regime for well studied learning strategies [Matias *et al.*, 2015].

Acknowledgments

M. Copelli is grateful for the hospitality during a visit to Gabriel Mindlin's lab at the University of Buenos Aires in December of 2017, and acknowledges financial support from Brazilian agencies CNPq (Grant 310712/2014-9), CAPES (Grant PVE 88881.068077/2014-01) as well as FAPESP Center for Neuromathematics (Grant 2013/07699-0, S. Paulo Research Foundation).

Funding

This work describes research partially funded by National Council of Scientific and Technical Research (CONICET), National Agency of Science and Technology (ANPCyT), University of Buenos Aires (UBA) and National Institute of Health through R01-DC-012859.

References

Aihara, K., Matsumoto, G. & Ikegaya, Y. [1984] "Periodic and non-periodic responses of a periodically forced Hodgkin–Huxley oscillator," *J. Theoret. Biol.* **109**, 249–269.

Alonso, R. G., Trevisan, M. A., Amador, A., Goller, F. & Mindlin, G. B. [2015] "A circular model for song motor control in serinus canaria," *Front. Comput. Neurosci.* **9**, 41.

Amador, A., Perl, Y. S., Mindlin, G. B. & Margoliash, D. [2013] "Elemental gesture dynamics are encoded by song premotor cortical neurons," *Nature* **495**, 59.

Ashmore, R. C., Wild, J. M. & Schmidt, M. F. [2005] "Brainstem and forebrain contributions to the generation of learned motor behaviors for song," *J. Neurosci.* **25**, 8543–8554.

Bera, B. K., Majhi, S., Ghosh, D. & Perc, M. [2017] "Chimera states: Effects of different coupling topologies," *Europhys. Lett.* **118**, 10001.

Coombes, S., Owen, M. R. & Smith, G. [2001] "Mode locking in a periodically forced integrate-and-fire-or-burst neuron model," *Phys. Rev. E* **64**, 041914.

Dima, G. C., Goldin, M. & Mindlin, G. B. [2018] "Modeling temperature manipulations in a circular model of birdsong production," *Papers in Phys.* **10**, 100002.

Hoppensteadt, F. C. & Izhikevich, E. M. [2012] *Weakly Connected Neural Networks*, Vol. 126 (Springer Science & Business Media).

Huygens, C. [1893] "Oeuveres completes de Christian Huygens," Includes correspondence from 1665, Vol. 5 (Martinus, Nijhoff, The Hague, Netherlands).

Majhi, S., Perc, M. & Ghosh, D. [2016] "Chimera states in uncoupled neurons induced by a multilayer structure," *Scient. Rep.* **6**, 39033.

Majhi, S., Perc, M. & Ghosh, D. [2017] "Chimera states in a multilayer network of coupled and uncoupled neurons," *Chaos* **27**, 073109.

Matias, F. S., Carelli, P. V., Mirasso, C. R. & Copelli, M. [2011] "Anticipated synchronization in a biologically plausible model of neuronal motifs," *Phys. Rev. E* **84**, 021922.

Matias, F. S., Carelli, P. V., Mirasso, C. R. & Copelli, M. [2015] "Self-organized near-zero-lag synchronization induced by spike-timing dependent plasticity in cortical populations," *PLoS One* **10**, e0140504.

Matias, F. S., Gollo, L. L., Carelli, P. V., Mirasso, C. R. & Copelli, M. [2016] "Inhibitory loop robustly induces anticipated synchronization in neuronal microcircuits," *Phys. Rev. E* **94**, 042411.

Nottebohm, F., Stokes, T. M. & Leonard, C. M. [1976] "Central control of song in the canary, serinus canarius," *J. Comparat. Neurol.* **165**, 457–486.

Okubo, T. S., Mackevicius, E. L., Payne, H. L., Lynch, G. F. & Fee, M. S. [2015] "Growth and splitting of neural sequences in songbird vocal development," *Nature* **528**, 352.

Pikovsky, A., Rosenblum, M. & Kurths, J. [2003] *Synchronization*: *A Universal Concept in Nonlinear Sciences*, Vol. 12 (Cambridge University Press).

Pyragienė, T. & Pyragas, K. [2013] "Anticipating spike synchronization in nonidentical chaotic neurons," *Nonlin. Dyn.* **74**, 297–306.

Sun, X. & Li, G. [2017] "Synchronization transitions induced by partial time delay in a excitatory–inhibitory coupled neuronal network," *Nonlin. Dyn.* **89**, 2509–2520.

Sun, X., Perc, M. & Kurths, J. [2017] "Effects of partial time delays on phase synchronization in Watts–Strogatz small-world neuronal networks," *Chaos* **27**, 053113.

Voss, H. U. [2000] "Anticipating chaotic synchronization," *Phys. Rev. E* **61**, 5115.

Wang, Q., Duan, Z., Perc, M. & Chen, G. [2008] "Synchronization transitions on small-world neuronal networks: Effects of information transmission delay and rewiring probability," *Europhys. Lett.* **83**, 50008.

Wang, Q., Perc, M., Duan, Z. & Chen, G. [2009] "Synchronization transitions on scale-free neuronal networks due to finite information transmission delays," *Phys. Rev. E* **80**, 026206.

Wang, Q. & Chen, G. [2011] "Delay-induced intermittent transition of synchronization in neuronal networks with hybrid synapses," *Chaos* **21**, 013123.

Wang, Q., Chen, G. & Perc, M. [2011] "Synchronous bursts on scale-free neuronal networks with attractive and repulsive coupling," *PLoS One* **6**, e15851.

Wilson, H. R. & Cowan, J. D. [1973] "A mathematical theory of the functional dynamics of cortical and thalamic nervous tissue," *Kybernetik* **13**, 55–80.